Electrochemical Modulation of Photonic Metamaterials

By *Li-Hua Shao, Matthias Ruther,* Stefan Linden, Sabine Essig, Kurt Busch, Jörg Weissmüller,* and *Martin Wegener*

Most metamaterials rely on resonances of metallic split-ring resonators[1] that can give rise to an effective magnetic response at elevated or even at optical frequencies.[2,3] For many applications, it would obviously be highly desirable to tune these metamaterial resonances or to even modulate them, ideally by an electric signal. Several approaches have recently been discussed. This includes using liquid crystals,[4–6] drops of silicon-nanospheres/ethanol solution,[7] optically pumped silicon at THz frequencies,[8] phase transitions in VO_2,[9,10] and phase-change materials.[11] An appealing route that is particular for metallic metamaterials is to directly modify the metal optical properties via the metal's charge density by an applied electric potential. Along these lines, field-effect-transistor like structures have recently been discussed at far-infrared frequencies[12,13] as well as at optical frequencies.[14] Even before many of these studies, electrochemically induced modulation of the metal's surface charge density has been demonstrated, e.g., in the context of mechanical properties.[15,16] Corresponding changes of the metal's optical properties have been investigated on bulk Au, Ag, and Cu single crystal surfaces,[17] on surface plasmon polaritons of thin Au films,[18] as well as on particle plasmon resonances of Au nanocrystals.[19] However, for bulk Au crystals,[17] the resulting optical modulation of the reflectance has been less than 1%. The observed effects have also been quite small for the case of surface plasmon polaritons. On the other end, for chemically synthesized Au nanocrystals, the modulation of the optical properties could even be seen by a color change with the naked eye in dark-field microscopic images.[19] Thus, it has not been clear at all whether sizable electrochemical optical modulation could be translated to lithographically fabricated metallic optical metamaterials. Their relevant feature sizes tend to be intermediate to bulk crystals on the one end and nanocrystals on the other end. The optical properties of metal nanocrystals can often be treated within the electrostatic limit, whereas those of most metamaterial building blocks such as split-ring resonators cannot. Hence, the metamaterial resonances for, e.g., using Au as the constituent metal, are well separated from the metal's interband transitions, whereas the plasmonic resonances are quite close to the onset of the metal's interband transitions for nanocrystals within the electrostatic limit. All these aspects make our work on electromodulation of photonic metamaterials reported in this Letter distinct from previous work. Moreover, we show in this Letter that the resulting electrochemical modulation is surprisingly large and hence attractive for applications.

In our electrochemical experiments, we employ arrays of gold split-ring resonators[20] (SRR). Each array has a footprint of 80 μm × 80 μm. An example of a 10-nm thin gold structure is shown in the inset in **Figure 1a**. The SRR arrays have been fabricated using a lift-off procedure following standard electron-beam lithography[20] on glass substrates coated with a 10-nm thin film of indium tin oxide (ITO) and a 2 to 3-nm thin Cr film as adhesion promoter. Additional results (not shown here) were obtained with a series of samples deposited without the Cr layer. These samples tended to detach after repeated electrochemical cycles, but results were otherwise consistent with those obtained with the Cr layer. All films (ITO, Cr, and Au) are made using high-vacuum electron-beam deposition. Gold is deposited at a rate of 0.1 nm/s. The average film thicknesses are determined by atomic-force microscopy (AFM). The ITO provides the contact to the gold nanostructures, which form the working electrode in our electro-modulation experiments (for details of the electrochemical setup see Experimental Section).

The electrochemical processes at the gold surface under the conditions of our experiment can be identified based on the cyclic voltammograms of current versus potential, U, during cyclic scans of U (Figure 1a). The most distinctive feature is a peak at positive potential that occurs only during the first scan. This peak is absent if no Cr adhesion layer is used (not depicted). Thus, this peak can be linked to partial dissolution of Cr. In the subsequent cycles, peaks in the potential range $U > 0$ correspond to the reversible adsorption and desorption of oxygen species not exceeding one adsorbed monolayer. We estimate a corresponding variation of the surface charge density of

[*] L.-H. Shao,[+] M. Ruther,[+] Prof. S. Linden,[+] Prof. J. Weissmüller, Prof. M. Wegener
Institut für Nanotechnologie
Karlsruhe Institute of Technology (KIT)
Postfach 3640, D-76021 Karlsruhe (Germany)
E-mail: matthias.ruther@kit.edu
L.-H. Shao, M. Ruther, Prof. S. Linden, S. Essig, Prof. K. Busch, Prof. J. Weissmüller, Prof. M. Wegener
DFG-Center for Functional Nanostructures (CFN)
Karlsruhe Institute of Technology (KIT)
D-76131 Karlsruhe (Germany)
M. Ruther, Prof. S. Linden, Prof. M. Wegener
Institut für Angewandte Physik
Karlsruhe Institute of Technology (KIT)
Wolfgang-Gaede-Strasse 1, D-76128 Karlsruhe (Germany)
S. Essig, Prof. K. Busch
Institut für Theoretische Festkörperphysik
Karlsruhe Institute of Technology (KIT)
Wolfgang-Gaede-Strasse 1, D-76128 Karlsruhe (Germany)
Prof. S. Linden
Current Address: Physikalisches Institut, Universität Bonn, Nußallee 12, D-53113 Bonn (Germany)
[+] These authors have contributed equally to this work

DOI: 10.1002/adma.201002734

ADVANCED MATERIALS
www.advmat.de

www.MaterialsViews.com

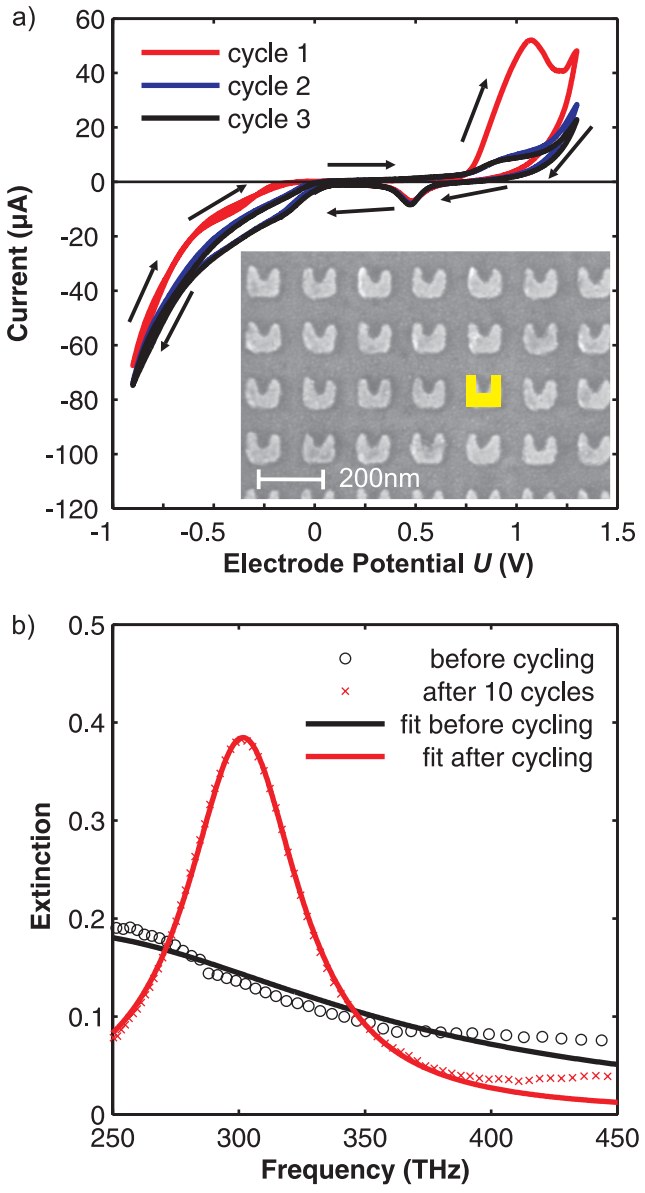

Figure 1. a) Typical cyclic voltammograms of an array of 10-nm thin gold split-ring resonators (scanning electron micrograph shown as inset) in a NaF-based aqueous electrolyte for electrode potentials ranging from –0.9 to +1.3 V. The first cycle is shown in red, the second in blue, and the third in black. Further cycles coincide within the linewidth of the curves. b) Corresponding normal-incidence extinction spectra for vertical incident linear polarization of light and for open-circuit conditions before (black symbol) and after $N = 10$ complete cycles (red symbol). The solid curves represent Lorentzian fits to the measured data. Note the very substantial sharpening of the resonance.

1.7 electron per surface gold atom, consistent with literature.[21] The large current values at $U < 0$ indicate Faraday reactions related to oxygen trace contaminants in the open cell.

Extinction spectra are shown in Figure 1b. As usual, the extinction is defined as the negative logarithm of the intensity transmittance, i.e., unity extinction corresponds to a suppression of the transmittance by one order of magnitude. In these experiments, the full opening angle of the cone of light is 5 degrees, approximating very nearly normal-incidence conditions. Normalization of the transmittance spectra is with respect to the bare ITO-coated substrate, i.e., without the Cr/Au nanostructures, in the same electrochemical cell (5 mm electrolyte thickness). In this fashion, the optical properties of the electrochemical cell drop out. The transmittance of the entire electrochemical cell is about 50% (not shown). This means that the electrolyte absorption does not significantly affect the plasmonic damping. After completion of sample fabrication, the 10-nm thin gold structures show only a very broad plasmonic resonance–in air as well as in the electrolyte. This is not surprising in view of the very large gold electron scattering/damping due to the considerable surface roughness and presence of grain boundaries expected for such very thin evaporated amorphous gold films. However, after 10 electrochemical cycles over a range from –0.9 V to +1.3 V – which we will call the "training" phase in what follows–a much more pronounced and sharper plasmonic resonance appears (for thicker gold films, the plasmonic resonances exhibit low damping even without initial electrochemical cycling.[20]) This extinction resonance centered at around 300 THz frequency in Figure 1b corresponds to a higher-order resonance of the SRR that can be excited for vertical incident linear polarization of light.[20] The measured extinction spectra can be well fitted by Lorentzians, providing us with the resonance position (±0.5 THz) and the resonance half-width-at-half-maximum (or damping). In Figure 1b, the extracted damping reduces from more than 100 THz to 27 THz. This training effect clearly correlates with the change in the cyclic voltammogram after the first complete cycle and it is only observed if the scan includes potentials $U > 0.9$ V. We tentatively assign the training effect to an enhanced mobility of gold atoms associated with a transient increase in surface diffusivity during the lifting of the oxygen adsorbate layer[21,22] at the positive end of the potential scale. The training effect also reproducibly persists once the nanostructure is removed from the electrolyte, making it useful as a simple electrochemical post-processing step for metamaterial fabrication. This approach complements recent work in a different size and thickness regime based on thermal annealing.[23]

Once the plasmonic resonance is established by electrochemical training, it also persists within the electrolyte, allowing for further studies. The resulting extinction spectra for one complete cycle and for a rather large electrode-potential window ranging from –0.9 V to +1.3 V are shown in **Figure 2a**. Obviously, the resonance exhibits a substantial red shift with respect to zero bias for positive potentials and a blue shift for negative potentials. Altogether, the peak of the extinction spectrum shifts by as much as 55 THz within one cycle, which is about 18% of the center frequency or more than twice the damping for zero electrode potential (24 THz). For example, the reduction of the extinction spectrum peak of 0.42 (at 50 mV) to 0.14 (at 1300 mV) at 318 THz frequency corresponds to a change of the transmittance from 38% to 72%, i.e., a change of transmittance by about a factor of two. In addition to this shift, the resonance damping also varies with potential. It increases from 24 THz at $U = 0.05$ V to 31 THz at $U = +1.3$ V and to 36 THz at $U = -0.9$ V. Further extinction data for two complete cycles are shown as a false-color plot in Figure 2b.

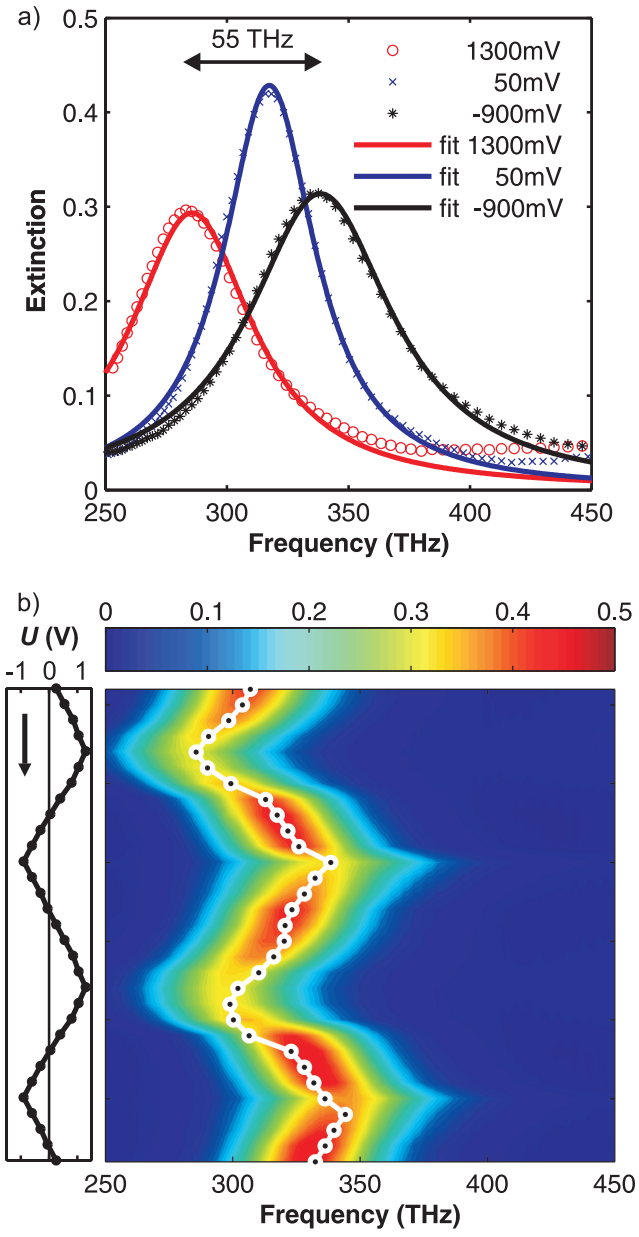

Figure 2. The electrode potential is varied in a window ranging from –0.9 to +1.3 V (compare Figure 1a)). a) Three selected extinction spectra from one electrochemical cycle taken after $N = 10$ training cycles. The solid curves are Lorentzian fits to the data, the observed peak-to-peak frequency shift of 55 THz is indicated. b) Further extinction spectra plotted on a false-color scale for two complete electrochemical cycles (2 hours acquisition time, time runs from top to bottom) under the same conditions as a). The electrode potential varies as shown on the left-hand side; the dots correspond to the actually measured values. The white dots in the false-color plot indicate the resonance center frequencies as obtained from the Lorentzian fits.

While the modulation of the gold surface-charge density is expected to be a reversible effect, the electrochemical training as described above is clearly irreversible. It is also obvious from Figure 2b that the resonance position after two cycles does not quite recover its original position. This raises the question what fraction of the 55-THz frequency shift in Figure 2a is reversible and what fraction is irreversible. To address this important question, we cycle the electrode potential several times for two smaller electrode-potential windows while observing the extinction spectra for similar samples. The resulting resonance positions (as extracted from the Lorentzian fitting) are summarized in the left-hand side column of **Figure 3**, the dampings in the right-hand side column. Following the above 10-cycles training procedure, we start with the small electrode-potential window ranging from –0.5 V to +0.9 V shown in Figure 3a. The three depicted complete cycles reveal little if any irreversible effect.

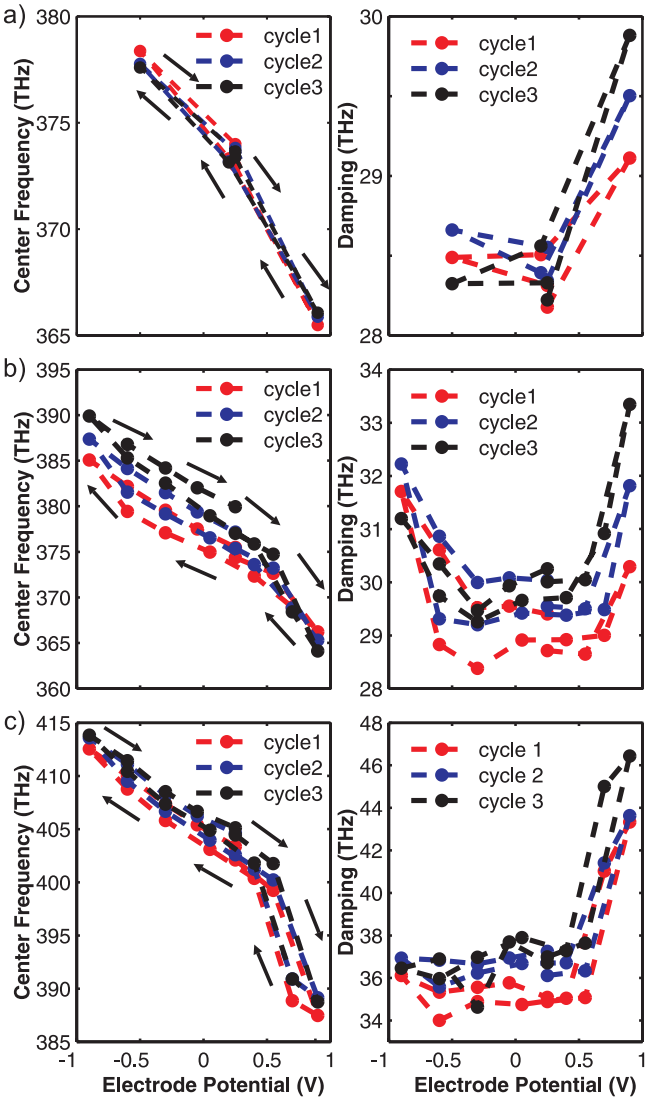

Figure 3. Split-ring-resonator resonance positions (left-hand side colum) and dampings (right-hand side columns) as obtained from Lorentzian fits to the measured data as in Figure 2 for three complete electrode-potential cycles in each sub-panel, a)–c). The gold film thickness is 10 nm. a) Electrode-potential window ranging from –0.5 V to +0.9 V and immediately after the original $N = 10$ training cycles. b) Following the measurements shown in a) and for a larger electrode-potential window ranging from –0.9 V to +0.9 V. c) Following b) and an additional 100 cycles, i.e., $N = 110$. Note that, for the conditions of a) and c) very nearly reversible electrochemical modulation of the optical resonance positions is obtained.

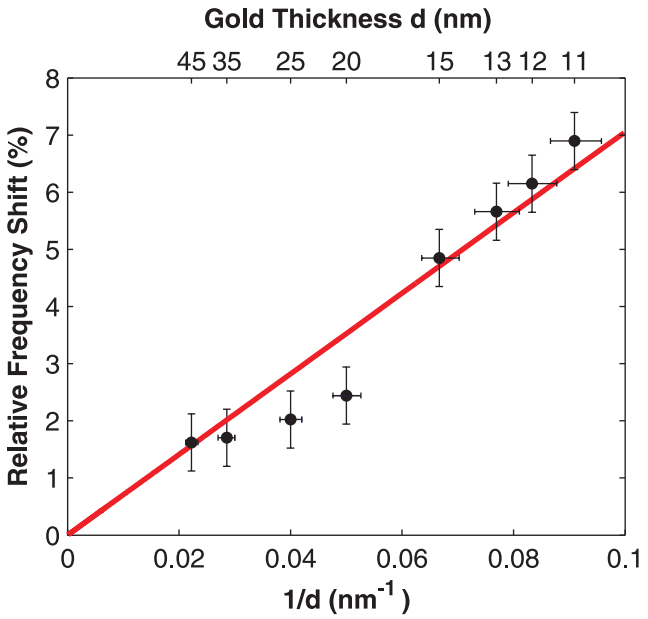

Figure 4. Relative split-ring-resonator resonance frequency modulation (i.e., ratio of frequency shift and center frequency for zero electrode potential) as obtained from Lorentzian fits to the measured data as in Figure 2 versus the inverse, $1/d$, of the gold thickness. In all cases, after the initial electrochemical training, the electrode-potential is varied in the range from –0.9 V to +0.9 V following $N = 100$ electrochemical cycles. Obviously, the reversible modulation is more pronounced for thin gold structures due to their larger surface-to-volume ratio. The red graph is a straight line of best fit $\propto 1/d$.

Next, the electrode-potential window is increased from –0.9 V to +0.9 V in Figure 3b. Obviously, the modulation becomes somewhat hysteretic and exhibits a drift towards higher frequencies, i.e., the resonance does not quite come back to the same position after one cycle. However, this irreversible part essentially saturates after another 100 cycles under the same conditions as shown in Figure 3c. Here, we obtain reversible frequency shifts as large as 25 THz–which is still comparable to the resonance damping for zero electrode potential (35 THz for this sample). We assign the irreversible contributions to structural changes similar to those during the initial training.

To further test our overall interpretation, we have performed additional experiments in which the gold film thickness of the SRR is varied systematically. Clearly, we expect smaller reversible frequency shifts from surface-charge effects for thicker Au films due to the less favorable surface-to-volume ratio. Results of corresponding experiments are shown in **Figure 4**. As expected, for a given voltage modulation within the reversible regime, the observed frequency swing decreases with increasing gold thickness d of the SRR, approximately proportional to $1/d$. Finally, the experimental observations are in qualitative agreement with simple numerical modeling (see **Experimental Section**) where the extra electronic charge in the space-charge layer at the metal side of the metal-electrolyte interface is modeled in terms of an extra layer of metal, increment the net number of conduction electrons in the structure.

In conclusion, we have shown that sizable reversible tuning and modulation of plasmonic resonances in optical metamaterials is possible by electrochemical modulation, making this approach an attractive alternative to other existing techniques.

Experimental Section

Experiment: The electrochemical cell is a quartz glass cuvette filled with a 0.7 M solution of NaF (Suprapur, Merck) in ultrapure 18.2 MΩ cm grade water (Arium 611, Sartorius) and open to air. Cleaning procedures are analogous to Ref.[24] The metamaterial sample is immersed in the solution and its potential–as measured relative to a standard reference electrode (RE), Ag/AgCl in saturated KCl solution–is controlled by a commercial potentiostat (VoltaLab PST 050, Radiometer Analytical). In this fashion we can reproducibly control the electrode potential and specify its value at an absolute scale. The RE is no leakage at all, which means there should not be Cl^- contamination. Optical spectra were recorded at constant potential, after the decay of the initial charging current transient. We use a macroscopic gold spiral as the counter electrode within the electrolyte. The aqueous electrolyte is opaque in the near-infrared (i.e., for wavelengths larger than 1.4 µm, equivalent to frequencies below 214 THz). Hence, we have chosen the SRR sizes such that the resonances of interest lie in the near-infrared part of the electromagnetic spectrum. This leads to SRR side lengths on the order of 100 nm (see inset in Figure 1a).

Numerical modeling: A recent density-functional-theory study[25] of charged Au surfaces suggests that the potential variation affects the electron density exclusively within the topmost atomic layer at the surface. Furthermore, the position of the image plane changes in good agreement with the notion of an electron liquid in which the charge density is a constant and the extra charge is accommodated by an outward shift of the surface of the electron liquid. This motivates us to view the modulation of the metal's surface charge, naively, as an effective change of the SRR metal-film thickness. To support this reasoning and to rule out others, we have performed numerical calculations based on a scattering-matrix approach (also known as Fourier Modal Method (FMM) or Rigorous Coupled Wave Analysis (RCWA)). To allow for quantitatively reliable results for only minute changes in the system parameters, great care regarding convergence of the numerical results has to be exerted. As a matter of fact, we find that even for grid-aligned SRR structures only the use of adaptive coordinates, either in analytical form[26] or automatically generated as in our work, leads to converged results. The gold is described by the free-electron Drude model with plasma frequency $\omega_{pl} = 1.37 \times 10^{16}$ s^{-1} and collision frequency $\omega_{coll} = 1.2 \times 10^{14}$ s^{-1}. For simplicity, the ITO film and the Cr adhesion layer are neglected. The glass substrate refractive index is taken as 1.45. The lateral dimensions of the SRR in the array are indicated in yellow in the inset in Figure 1a, the gold film thickness is $d = 10$ nm. Based on these parameters, we find numerically that a change in the SRR free-electron gas thickness by 1 nm (i.e., from 10 nm to 11 nm) leads to a blue shift of the resonance of 12.3 THz. The relative frequency shift decreases for thicker SRR like $\propto 1/d$. This behavior qualitatively reproduces our experimental observations. In order to obtain the same blue shift of 12.3 THz for a fixed thickness of $d = 10$ nm, the refractive index of the entire electrolyte would have to exhibit a large change from 1.33 to 1.24. Similarly, if the index was only modulated within a 1-nm thin surface layer within the electrolyte, the local index of this surface layer would need to decrease from 1.33 to 0.35. Even when changes in the pH of the electrolyte–for instance as the result of the oxygen reduction reaction at the negative end of the potential scale–are allowed for, changes of the refractive index of this magnitude can be ruled out in our experiments. Hence, these alternative mechanisms might play a certain role but they are quite unlikely to dominate in our experiments. A more detailed theory would have to treat the electrochemical processes at the gold surface on the atomic scale. Unfortunately, however, such theory describing the influence on the optical properties is presently not available.

Acknowledgements

We thank Costas M. Soukoulis for stimulating discussions. We acknowledge financial support provided by the Deutsche Forschungsgemeinschaft (DFG) and the State of Baden-Württemberg through the DFG-Center for Functional Nanostructures (CFN) within subprojects A1.1, A1.5, and A1.6. The project PHOME acknowledges the financial support of the Future and Emerging Technologies (FET) programme within the Seventh Framework Programme for Research of the European Commission, under FET-Open grant number 213390. The project METAMAT is supported by the Bundesministerium für Bildung und Forschung (BMBF). The research of S.L. is further supported through a "Helmholtz-Hochschul-Nachwuchsgruppe" (VH-NG-232). The PhD education of M.R. and S.E. is embedded in the Karlsruhe School of Optics & Photonics (KSOP).

Received: July 29, 2010
Published online: October 11, 2010

[1] J. B. Pendry, A. J. Holden, D. J. Robbins, W. J. Stewart, *IEEE Trans. Microwave Theory Tech.* **1999**, *47*, 2075.
[2] V. M. Shalaev, *Nature Photon.* **2007**, *1*, 41.
[3] C. M. Soukoulis, S. Linden, M. Wegener, *Science* **2007**, *315*, 47.
[4] D. H. Werner, D.-H. Kwon, I.-C. Khoo, *Opt. Express* **2007**, *15*, 3342.
[5] X. Wang, D.-H. Kwon, D. H. Werner, I.-C. Khoo, A. V. Kildishev, V. M. Shalaev, *Appl. Phys. Lett.* **2007**, *91*, 143122.
[6] F. Zhang, L. Kang, Q. Zhao, J. Zhou, X. Zhao, D. Lippens, *Opt. Express* **2009**, *17*, 4360.
[7] T. Driscoll, G. O. Andreev, D. N. Basov, S. Palit, S. Y. Cho, N. M. Jokerst, D. R. Smith, *Appl. Phys. Lett.* **2007**, *91*, 062511.
[8] H.-T. Chen, J. F. O'Hara, A. K. Azad, A. J. Taylor, R. D. Averitt, D. B. Shrekenhamer, W. J. Padilla, *Nature Photon.* **2008**, *2*, 295.
[9] M. J. Dicken, K. Aydin, I. M. Pryce, L. A. Sweatlock, E. M. Boyd, S. Walavalkar, J. Ma, H. A. Atwater, *Opt. Express* **2009**, *17*, 18330.
[10] H.-T. Driscoll, B.-G. Kim, B.-J. Chae, Y.-W. Kim, N. M. Lee, S. Jokerst, D. R. Palit, D. R. Smith, M. Di Ventra, D. N. Basov, *Science* **2009**, *325*, 1518.
[11] Z. L. Samson, K. F. Mac Donald, F. D. Angelis, B. Gholipour, K. Knight, C. C. Huang, E. D. Fabrizio, D. W. Hewak, N. I. Zheludev, *Appl. Phys. Lett.* **2010**, *96*, 143105.
[12] H. T. Chen, W. J. Padilla, J. M. O. Zide, A. C. Gossard, A. J. Taylor, R. D. Averitt, *Nature* **2006**, *444*, 597.
[13] H. T. Chen, W. J. Padilla, M. J. Cich, A. K. Azad, R. D. Averitt, A. J. Taylor, *Nature Photon.* **2009**, *3*, 148.
[14] E. Feigenbaum, K. Diest, H. A. Atwater, *Nano Lett.* **2010**, in press.
[15] J. Weissmüller, R. N. Viswanath, D. Kramer, P. Zimmer, R. Wurschum, H. Gleiter, *Science* **2003**, *300*, 312.
[16] H.-J. Jin, X.-L. Wang, S. Parida, K. Wang, M. Seo, J. Weißmüller, *Nano Lett.* **2010**, *10*, 187.
[17] R. Kötz, D. M. Kolb, *Z. Physik. Chemie NF* **1978**, *112*, 69.
[18] J. C. Abanulo, R. D. Harris, P. N. Bartlett, J. S. Wilkinson, *Appl. Opt.* **2001**, *40*, 6242.
[19] C. Novo, A. M. Funstone, A. K. Gooding, P. Mulvaney, *J. Am. Chem. Soc.* **2009**, *131*, 14664.
[20] S. Linden, C. Enkrich, M. Wegener, J. F. Zhou, T. Koschny, C. M. Soukoulis, *Science* **2004**, *306*, 1351.
[21] B. E. Conway, *Prog. Surf. Sci.* **1995**, *49*, 331.
[22] C. M. Vitus, A. J. Davenport, *J. Electrochem. Soc.* **1994**, *141*, 1291.
[23] K. P. Chen, V. P. Drachev, J. D. Borneman, A. V. Kildishev, V. M. Shalaev, *Nano Lett.* **2010**, *10*, 916.
[24] M. Smetanin, R. N. Viswanath, D. Kramer, D. Beckmann, T. Koch, L. A. Kibler, D. M. Kolb, J. Weißmüller, *Langmuir* **2008**, *24*, 8561.
[25] Y. Umeno, C. Elsässer, B. Meyer, P. Gumbsch, J. Weissmüller, *Europhys. Lett.* **2008**, *84*, 13002.
[26] T. Weiss, G. Granet, N. A. Gippius, S. G. Tikhodeev, H. Giessen, *Opt. Express* **2009**, *17*, 8051.